Journal of Biomedical Science (2007) 14:783–795
DOI 10.1007/s11373-007-9192-0

siRNA targeting midkine inhibits gastric cancer cells growth and induces apoptosis involved caspase-3,8,9 activation and mitochondrial depolarization

Qingling Wang, Yahong Huang, Yanhong Ni, Hui Wang & Yayi Hou*
Immunology and Reproductive Biology Lab, Medical School and State Key Laboratory of Pharmaceutical Biotechnology, Nanjing University, Nanjing, 210093, P.R. China

Received 29 January 2007; accepted 28 June 2007

Key words: midkine, gastric cancer, RNA interference, proliferation, apoptosis

Abstract

Midkine (MK), a heparin-binding growth factor, is expressed highly in various malignant tumors, so it acts as attractive therapeutic target. In the present study, we used siRNA targeting MK to downregulate human MK expression in human gastric cancer cell line BGC823 and SGC7901 so as to determine the advantages of this anticancer therapeutic. The cell proliferation was evaluated by a WST-8 (4-[3-(2-methoxy-4-nitrophenyl)-2-(4-nitrophenyl)-2H-5-tetrazolio]-1, 3-benzene disulfonate sodium salt) assay and colony formation assay. Apoptosis was determined by flow cytometer analysis and colorimetric assay. Our results showed that the BGC823 and SGC7901 cell growth were significantly inhibited by knockdown of MK gene. The loss of mitochondrial membrane potential, release of cytochrome c from the mitochondria into cytosol and increased activity of caspase-3, 8 and 9 occurred concomitantly with inhibition of MK gene. These results indicated that siRNA targeting MK gene can inhibit gastric cancer cells growth and induce apoptosis via mitochondrial depolarization and caspase-3 activation. MK siRNA may be a promising novel and potential therapeutic strategy for the treatment of gastric cancers.

Introduction

Midkine (MK), a heparin-binding growth factor, is detected in various human carcinoma specimens from pre-cancerous stages to advanced stages. It can act as an angiogenic, fibrinolytic and antiapoptotic factor in carcinoma cell lines, and induce the transformation of NIH/3T3, SW-13 and UN-UC-3 cells [1, 2]. MK is also detected in some normal human tissues. Results show that MK is highly expressed in the mucosal tissue of the small intestine, moderately in the thyroid, weakly in the tissues of the lung, colon, stomach, kidney, and spleen, and not at all in the liver [3]. Moreover, MK is expressed higher in human gastrointestinal cancers than in the corresponding non-cancerous tissues and normal tissue [3, 4]. Urinal-MK [5] and serum-MK levels increased in gastric cancer patients [6, 7], and serum-MK levels decreased after surgical resection of the tumor in several carcinomas, including gastric cancer [8]. MK may act as a prognostic marker for gastriointestinal stromal tumors [9]. Our previous study also shows that MK highly express in gastric cancer tissue from Chinese patients and the expressions of their mRNA and protein are all associated with the clinical stage and distant metastasis of gastric cancer in the Chinese patients [10]. These data suggest that MK may contribute to oncogenesis and tumor progression of gastric cancer, and can act as cancer bio-marker and therapy target.

Concerns have been raised recently about targeting MK used in disease therapy. Doxorubicin-conjugated anti-MK monoclonal antibody was reported as a potential anti-tumor drug [11]. Mouse MK antisense oligodeoxynucleotide demonstrated potent growth inhibitory effects on

*To whom correspondence should be addressed. Fax: +86-25-83686341; E-mail: yayihou@nju.edu.cn

rectal carcinoma growth *in vivo* [12]. Morpholino antisense oligomer targeting human MK exhibited a significant anticancer effect in the PC-3- and SW620-xenograft models [13]. Small interfering RNA targeting rabbit MK attenuates intimal hyperplasia in vein grafts [14]. Mouse MK antisense oligodeoxyribonucleotide inhibits renal damage induced by ischemic reperfusion [15].

RNA interference (RNAi) has become widely used as an experimental tool to analyze the function of mammalian genes, both *in vitro* and *in vivo*. Post-transcriptional gene expression can be mediated by small noncoding RNAs such as short interfering RNA (siRNA). siRNAs has been successfully applied for "loss-of-function" assays with resulting phenotypes in cultured cells and *in vivo* models [16–18]. However, siRNA targeting human MK used to gastric cancer therapy has not been reported to date. To develop an antitumor reagent, we designed human MK specific short interference RNA and examined their anticancer activity against gastric carcinoma cell lines BGC823 and SGC7901. In addition, the mechanism on MK inducing oncogenesis and tumor progression was analyzed.

Material and methods

Design of siRNA

Specific sequence for human MK Stealth™ Select RNA was designed and synthesized by Ivitrogen (Ivitrogen, Life Technologies, USA). Only one suitable sequence was selected. sense: 5'UGA AGAAGGCGCGCUACAAUGCUCA3', antisense: 5'UGAGCAUUGUAGCGCGCCUUCU UCA3'. Oligo Stealth ™ RNAi Negative Control Duplexes, which is designed to minimize sequence homology to any known vertebrate transcript, were obtained from Invitrogen.

Cell culture and transfection

BGC823 and SGC7901 cell lines were cultured in RPMI medium 1640 (Gibco/BRL) supplemented with 10% fetal bovine serum (Si Jiqing, China) at 37°C under 5% humidified CO_2 and 100 ug/ml each of streptomycin and penicillin G (Amresco). The siRNA was transfected using Lipofectamine 2000 (Ivitrogen) according to the manufacturer's instructions. Briefly, approximately $3–4 \times 10^4$ cells/well were grown overnight in 24-wells plate. When cells reached to 30–50% confluence, they were transfected with anti-MK siRNA (100 nM) and negative control siRNA (100 nM) in serum-free medium using Lipofectamine 2000. After incubation for 4 h at 37°C, 400 ul RPMI 1640 with 10% FBS was added.

RNA extraction and semiquantitative reverse transcription-polymerase chain reaction (RT-PCR)

Briefly, after siRNA transfection, total RNA was extracted using the TaKaRa RNAiso Reagent (TaKaRa, Japan) according to the manufacturer's instructions. RNA concentrations were quantified by spectrophotometer at 260 nm. A 2 ug of total RNA was reverse-transcribed using Revert Aid™ First Strand cDNA Synthesis Kit (Fermentas). After RT reaction, 2 ul of the incubation mixture was used as the template for the following PCR using 2×Taq Enzyme Mix kit (TianGen, China). Oligonucleotides used as primers were synthesized by Ivitrogen, for MK (385bp), forward primer: 5'AAAAAAGCTTATGAAAAAGAAAGATAA GGTGAAGAAG 3', reverse primer: 5' AAAA-GAATTCCTAGTCCTTTCCCTTCCCT 3; for bcl-2 (288 bp) forward primer: 5'AGCTGCACCT GACGCCCTTCACCGC 3', reverse primer: 5' AGGAGAAATCAAACAGAG 3'; for bax (295 bp) forward primer: 5' TGCTTCAG GGTTTCATCCAGG 3', reverse primer: 5' GCC TTGAGCACCAGTTTG 3; for β-actin (280 bp), forward primer: 5'CCACGAAACTACCTT-CAACTCC 3', reverse primer: 5'TCATACTC CTGCTGCTTGCTGATCC 3'. PCR was carried out for 30 cycles of denaturation (30 s at 94°C), annealing (40 s at 55°C), and extension (30 s at 72°C). The PCR products were then separated on 1% agarose gel containing 0.5 ug/ml ethidium bromide. The gel was put on an UV-transilluminator and photographed. The MK signal was measured by a densitometer and standardized against the β-actin signal using a digital imaging and analysis system.

Western blot analysis

BGC823 and SGC791 cells were seeded and transfected as the indicated above. Cells were lysed in 1%SDS, the total protein of samples was

adjusted to 100 ug/lane, and then the protein of samples was transfected to Poly-vinylidene fluoride membrane (Roche, Germany). Antibodies against MK (BA1263, 1:400; Boster, China), Cytochrome c (ANN0012, 1 ug/ml; Biovision, USA), β-actin (BA0410, 1:400; Boster, China) and HRP-conjugated goat anti-rabbit secondary antibody (BA1054, 1:2000; Boster, China) were used. Protein bands were detected using DAB solution (Boster, AR1022).

Preparation of mitochondrial and cytosolic extracts

Both mitochondrial and cytosolic extracts were prepared according to the instruction of Cytochrome *c* Releasing Apoptosis Assay Kit (Biovision, California, USA). Briefly, after treatment with or without transfection, 1.5×10^7cells were collected by centrifugation at 600*g* at 4°C for 5 min and then washed twice with ice-cold PBS. The cell pellets were resuspended in ice-cold homogenizing buffer, including DTT and protease inhibitors. After homogenization (40 strokes), the homogenates were centrifuged at 700*g* at 4°C for 10 min. Supernatant was collected and centrifuged at 10,000*g* at 4°C for 30 min. The supernatant was used as the cytosol fraction, and the pellet was resolved in lysis buffer as the membrane fraction. The supernatants and the pellets were analyzed by Western blotting, respectively.

Cell viability analysis

Cell viability was assessed with a Cell Counting Kit (Dojin Laboratories, Kumamoto, Japan) [19]. Briefly, BGC823 and SGC791 cells, transfected with anti-MK siRNA and negative control RNA, were plated in 96-well plates in RPMI 1640 supplemented with 10% FBS at a density of 3×10^3 cells/well. After 4 h, the medium was changed to serum-free medium, and the cells were cultured $\leq$ 5 days. 10 ul of solution containing WST-8 (4-[3-(2-methoxy-4-nitropheny[T1]l)-2-(4-nitrophenyl)-2H-5-tetrazolio]-1, 3-benzene disulfonate sodium salt) was added to each well and was incubated for an additional 4 h. The absorbance was measured at 450 nm on a muti-detection microplate reader (Hynergy^{TM} HT, BIO-TEK).

Colony formation analysis

To measure the cell colony formation ability, minimal concentrations of FBS (2%) were added to the medium. Briefly, BGC823 and SGC791 cells, transfected with anti-MK siRNA and negative control RNA, were plated in 6-well plates in RPMI 1640 supplemented with 10% FBS at a density of 1,000 cells/well. After 4 h, the medium was changed to FBS (2%) supplemented medium. After 10 days of incubation at 37°C in an incubator under a humidified 5% CO_2 atmosphere, cells were fixed 2 min with methanol, died 20 min with 1% crystal violet, and the numbers of colonies($\geq$50 cells) formed in the whole well were counted.

Analysis of hypodiploid cells

Analysis of hypodiploid cells was performed using PI staining [12]. In brief, BGC823 and SGC7901 cells subjected to 72 h after transfection were fixed in 75% ethanol for 2 h at room temperature. Then they were stained with propidium iodide staining buffer (Trixon X-100, EDTA, RNAse A, PI) for 10 min at dark. The fluorescence of PI was monitored by flow cytometer (Becton-Dickson, Immunocytometry System, San Jose, CA) with an excitation wavelength of 488 nm and an emission wavelength of 625 nm. Apoptotic cells were determined on a PI histogram as a hypodiploid. For each sample, 20,000 cells were analyzed. The data were analyzed using Cellquest software (Palo Alto, CA, USA).

Annexin V/PI staining

Cells were centrifuged to remove the medium, washed once with binding buffer (10 mM Hepes, 140 mM NaCl, 2.5 mM $CaCl_2$ in aquadest.) and stained with 5 ul Annexin V-FITC at RT for 15 min. 10 ul 20 ug/ml PI was added at RT for 10 min and cells analyzed by flow cytometry. Viable cells were negative for both PI and annexinV; apoptotic cells were positive for annexinV and negative for PI, whereas late apoptotic dead cells displayed both high annexin V and PI labeling. Non-viable cells which underwent necrosis were positive for PI and negative for annexin V.

Determination of the mitochondrial membrane potential by Rhodamine 123

Rhodamine 123 uptake by mitochondria is directly proportional to its membrane potential. BGC823 and SGC7901 cells subjected to 72 h after transfection were incubated with Rh 123 (5 ug/ml concentration) for 30 min in dark at 37°C. The cells were harvested and suspended in PBS. The mitochondrial membrane potential was measured by the fluorescence intensity (FL-1, 530 nm) of 10,000 cells on flow cytometer [20, 21].

Determination of active caspase-3, -8 and -9

In order to determine the potential role of the caspase- 3, -8 and -9 proteases in the pathways of MK knockdown - induced apoptosis, the activities of caspase- 3, -8 and -9 were measured by caspase-3, -8 and -9 Colorimetric Assay Kit (KeyGen, China) respectively. Briefly, 1×10^6 cells subjected to 72 h after transfection were lysed at 4°C for 30 min and the supernatant were transferred to a clean microfuge tube, protein concentration was assayed. Then, 50 ul 2×Reaction Buffer and 5 μl Caspase-3, 8, 9 Substrate were added, incubated at 37°C for 4 h in dark. The absorbance was measured at 405 nm on a muti-detection microplate reader (Hynergy^{TM} HT, BIO-TEK). The activity of caspase-3, 8, and 9 was determined by calculating the ratio of OD405 nm of transfected cells/OD 405 nm of parental cells following the instruction of the manufacturer.

Statistical analysis

Results were presented as the mean ± S.E.M. Statistical significance between groups was analyzed by one-way ANOVA followed by the Student–Newman–Keuls multiple comparisons tests. A p-value of < 0.05 was considered significant.

Results

siRNA targeting MK transfection down-regulates the corresponding mRNA and protein levels in BGC823 and SGC7901 cells

The efficacy of siRNA-mediated inhibition of MK synthesis in BGC823 and SGC7901 cells was analyzed by RT-PCR and Western blotting. As shown in Figure 1, when BGC823 and SGC7901 cells were transfected with the MK siRNA, MK mRNA (Figure 1a) and proteins (Figure 1c, d) were down-regulated 72 h later, but negative control siRNA didn't affect the MK mRNA and protein. β -actin mRNA and protein levels were also not affected by these siRNA.

Cell growth was inhibited by down-regulation of MK expression

To determine if suppression of MK was related to cell growth, cell viability was assessed with a Cell Counting Kit. The absorbance of MK siRNA-transfected BGC823 and SGC7901 cells was decreased significantly especially on day 4 and 5 after plated in 96-well plate. Negative siRNA showed no such effect (Figure 2a, b).

Furthermore, to test potential malignant state of the tumor cell line, colony-forming assay was conducted in BGC823 and SGC7901 cells transfected with MK siRNA or negative siRNA. The results showed that the colony numbers of cells transfected with MK siRNA were decreased by 4 to 5-fold, compared with parental cells and negative siRNA transfected cells (Figure 2c, d). These results showed that anti-MK siRNA had significant growth inhibition effect on BGC823 and SGC7901 cells.

Inhibiton of MK expression up-regulated cells apoptosis

To confirm suppression of MK expression induced apoptosis, the cells were stained with PI and analyzed for hypodiploid cells by flow cytometry. The fraction of cells in apoptosis was identified in a DNA histogram as a sub-G1 hypodiploid population. Figure 3 showed the hypodiploid sub-G1 phase in cells transfected with MK siRNA. The results exhibited that BGC823 and SGC7901 transfected with MK siRNA had sub-diploid peak and the percentage of cells with fragmented DNA increased compared with control. To further evaluate the induction of apoptosis, the cells were stained with annexin V and PI. A proportion of annexin V staining cells to the total MK siRNA-transfected cells was increased (Figure 4a, b). A little amount of necrotic cells which were stained with PI but not annexin V was also observed. Taken together, these results indicate that anti-

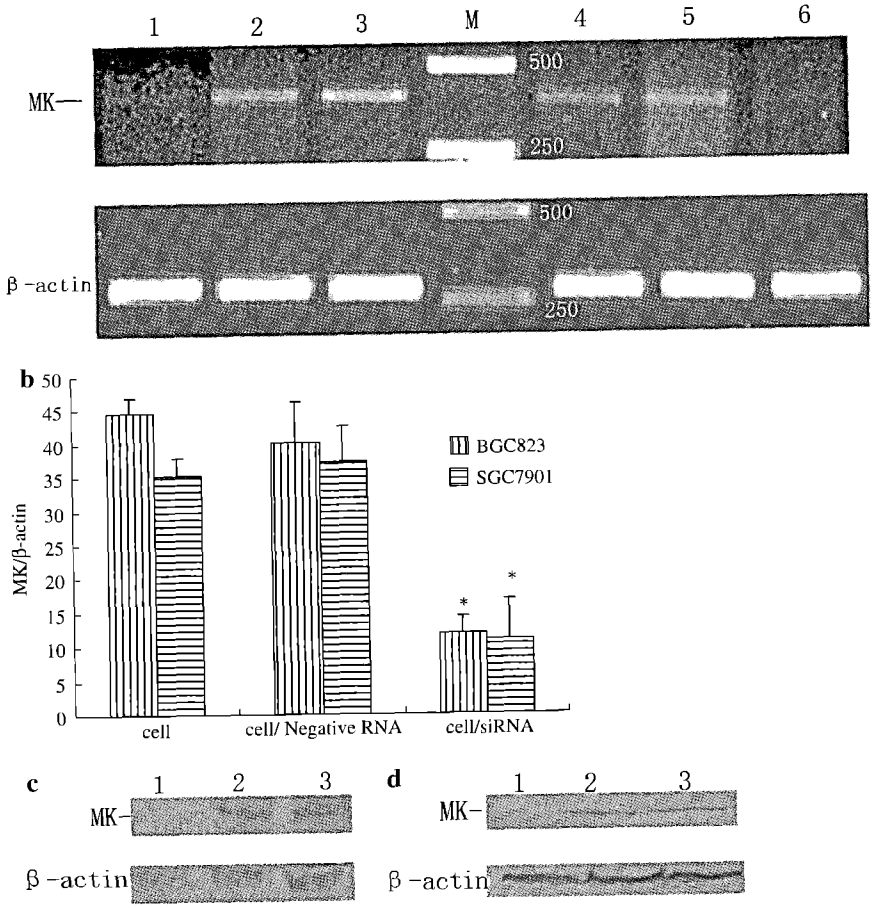

Figure 1. MK siRNA inhibited MK mRNA synthesis by RT-PCR and protein synthesis. (a) For mRNA analyses, the representative agarose gel electrophoresis of three independent experiments is shown. Lane 1: BGC823 transfected with 100 nM MK siRNA; lane 2: BGC823 transfected with 100 nM negative siRNA; lane 3: parent BGC823; lane 4: parent SGC7901; lane 5: SGC7901 transfected with 100 nM negative siRNA; lane6: SGC7901 transfected with 100 nM MK siRNA. (b) Densitometric analysis. The intensity of the band was scanned. The quotient of MK/β-actin gene was calculated. The data shown are the average of three independent experiments including cDNA synthesis and PCR analysis. The results are shown as mean ± S.E. from three representative independent experiments. * $p < 0.05$ versus Control. Western blots were performed to assay MK protein expression after siRNA treatment (c) BGC823 cells and (d) SGC7901 cells, Lane 1: cells transfected with 100 nM MK siRNA; lane 2: cells transfected with 100 nM negative siRNA; lane 3: parental cells.

MK siRNA induced BGC823 and SGC7901 cells apoptosis.

Inhibiton of MK expression decreased mitochondrial membrane potential

The loss of mitochondrial membrane potential is a hallmark for apoptosis. It is an early event coinciding with caspases activation. The effect of MK siRNA on the mitochondrial transmembrane potential was measured using rhodamine 123. The increase of percentages of apoptotic MK siRNA transfected cells was observed (Figure 5). Apoptotic cells in parental BGC823 and nagtive siRNA transfected BGC823 cells were approximately 4.15%, 7.13%. Apoptotic cells in parental SGC7901 and negative siRNA transfected SGC7901 cells were approximately 5.28 and 8.35%. However, the rate of apoptotic MK siRNA transfected cells increased to 32.15% in BGC823 and 36.99% in SGC7901.

Inhibiton of MK expression up-regulated expression of bax and down-regulated expression of bcl-2 and release of cytochrome c

Bcl-2 family proteins have a central role in controlling mitochondria apoptosome-mediated apoptotic pathway; the Bcl-2/Bcl-Xl subfamily proteins inhibit apoptosis, while the Bax/Bak subfamily promotes cell death [22, 23]. In this

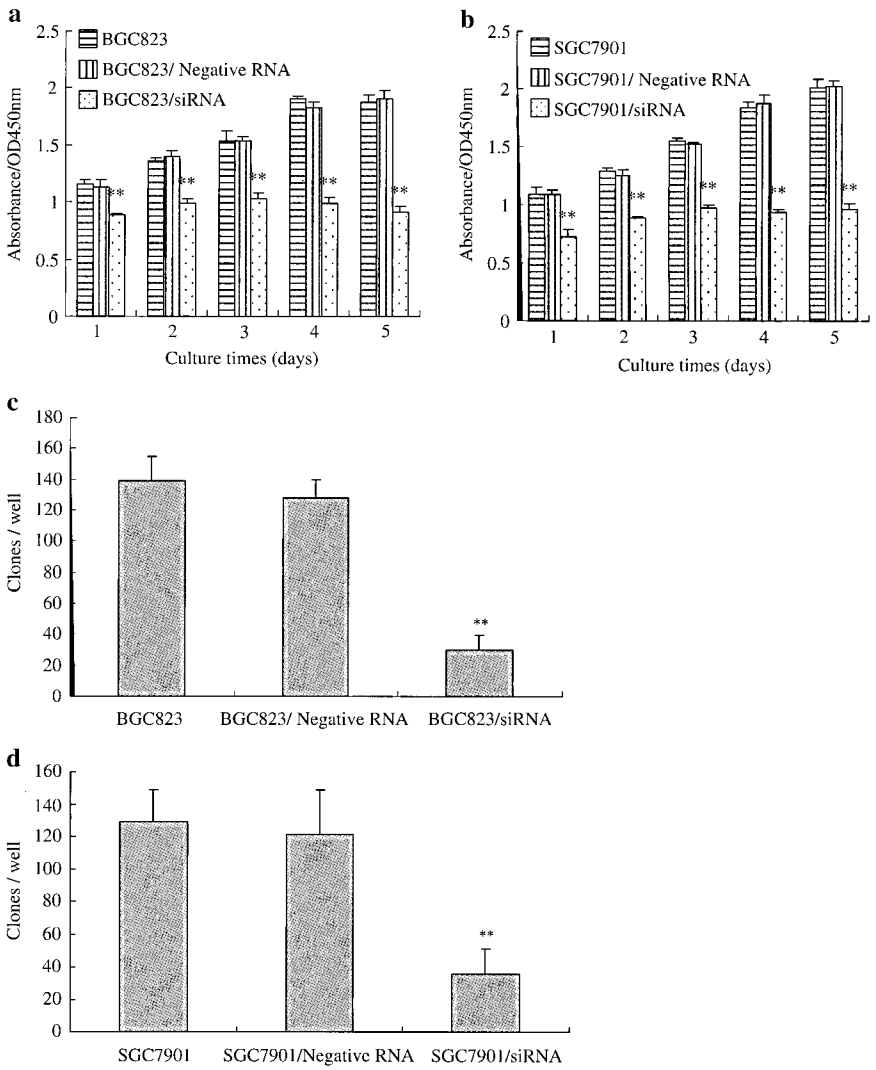

Figure 2. Effects of siRNA targeting MK on gastric cancer cell line BGC823 and SGC7901. (a and b) Inhibition of cell viability assayed with a Cell Counting kit every day for 5 days. Results were presented as the mean ± S.E.M from three independent experiments. * *, $p < 0.01$ versus control. (c and d) Colony formation. Cells were plated in 6-wells plate at a density of 1,000 cells/well, Number of colonies counted in triplicate with cell number ≥50 cells on 10th day. The results are presented as mean ± S.E with triplicate measurement. **$p < 0.01$ versus control.

study, we detected the bcl-2 and bax expression level by RT-PCR after siRNA target MK transfection (Figure 6). The mRNA expression of bcl-2 was decreased in BGC823 and SGC7901 after siRNA target MK transfection, while bax was increased.

Mitochondrial and cytosolic extracts were prepared according to the instruction of Cytochrome c Releasing Apoptosis Assay Kit (Biovision, California, USA). Figure 7 shows that after BGC823 and SGC7901 cells transfected with anti-MK siRNA, the release of cytochrome c from the mitochondria into cytosol was increased, compared with parental cells and cells transfected with negative RNA.

Activation of caspase-3, -8 and -9 via Inhibiton of MK expression

The caspase cascade is activated during apoptosis. Therefore, we examined the activity of caspase-3, 8 and 9 in BGC823 and SGC7901 transfected with MK siRNA or with negative RNA (Figure 8) by colorimetric assay. In addition to executioner

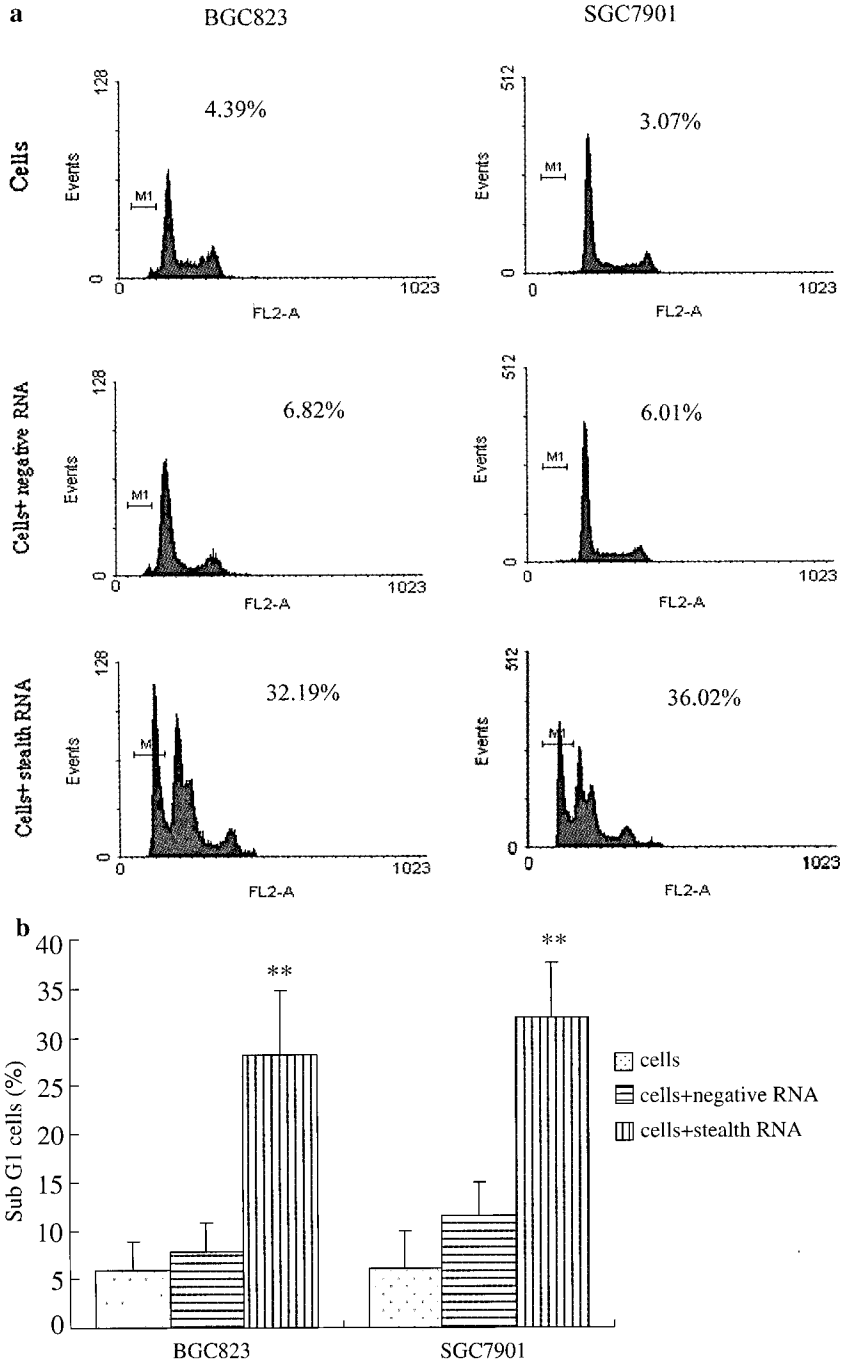

Figure 3. Hypodiploid cells were detected by flow cytometry. BGC823 and SGC7901 subjected to 72 h after transfection stained with PI, then hypodiploid cells was detected by flow cytometry. 20,000 cells were analyzed for each sample. (a) Sub-G1 cells were measured with a FACSCalibur flow cytometer and analyzed using Cellquest software as described in Material and methods. (b) Graph shows the percentages of Sub G1 cells which represent the mean ± S.E.M from three independent experiments. $^{**}p < 0.01$ versus control.

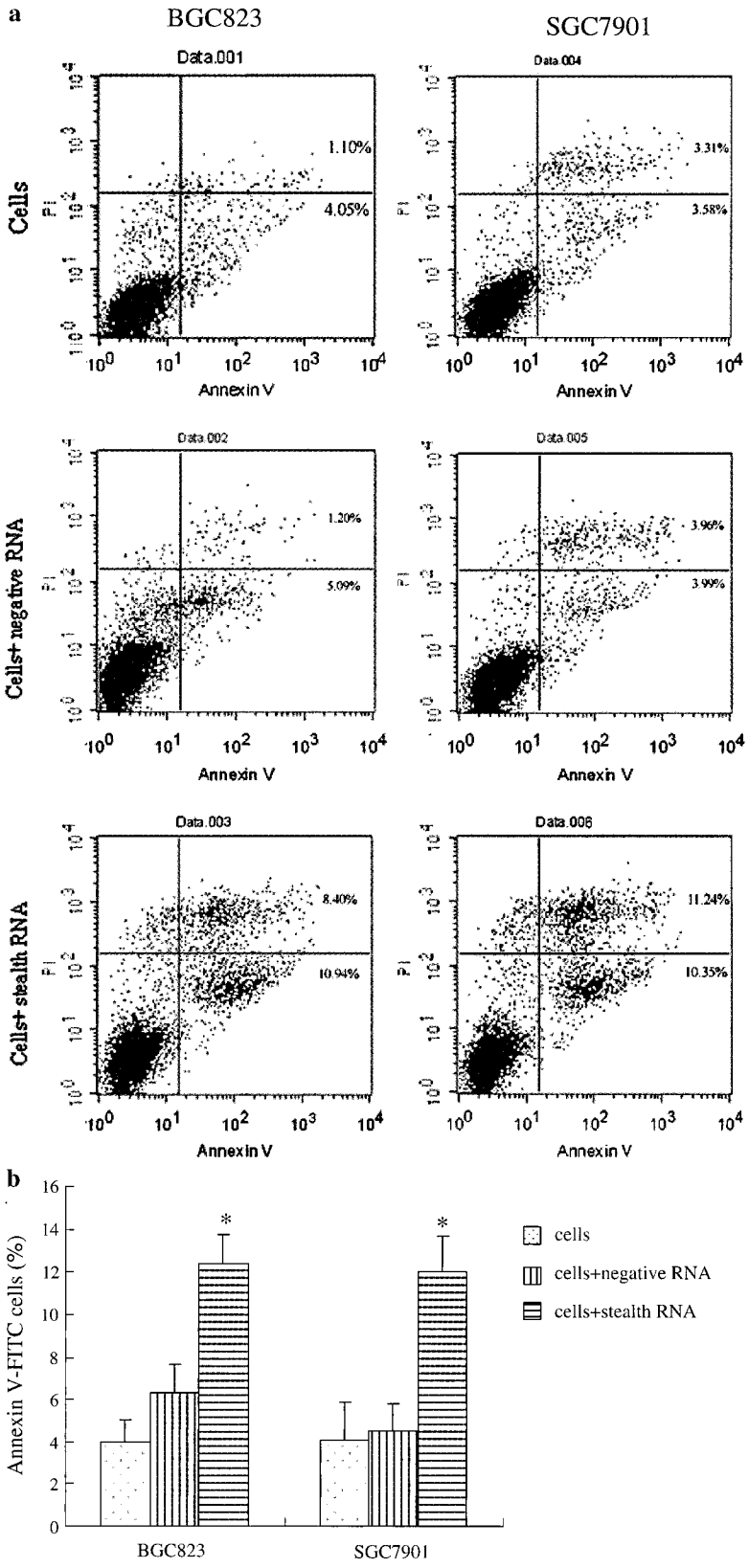
a
BGC823
SGC7901
Data.001
Data.004
Data.002
Data.005
Data.003
Data.006
Cells
Cells+ negative RNA
Cells+ stealth RNA
1.10%
4.05%
3.31%
3.58%
1.20%
5.09%
3.96%
3.99%
8.40%
10.94%
11.24%
10.35%
PI
Annexin V
b
Annexin V-FITC cells (%)
cells
cells+negative RNA
cells+stealth RNA
BGC823
SGC7901

◀ *Figure 4.* Effects of Anti-MK siRNA on BGC823 and SGC7901 cells discriminated by Annexin-V/PI double stain. (a) Representative dot plots of Annexin-V/PI staining are shown. The lower left quadrant contains the viable (double negative) population. The lower right quadrant contains the apoptotic (AnnexinV+/PI−) population. The upper left quadrant contains the necrosis (Annexin V-/PI+) population. The upper right quadrant contains the late apoptotic dead cells (Annexin V+/PI+). (b) Graph shows the percentages of Annexin V positive cells which represent the mean ± S.E.M from three independent experiments. $*p < 0.05$ versus control.

caspase-3, initiator caspase-8 and -9 are also important for apoptosis. The ratio of OD 405 nm of transfected cells/OD 405 nm of parental cells was calculated. In BGC823 cells, the value of caspase-3 and -9 reached about 5 and the value of caspase-8 just reached about 3. Similar result was obtained in SGC7901 cells.

Discussion

In this study, we found that MK siRNA could inhibit BGC823 and SGC7901 human gastric carcinoma cells growth, colony formation, induce apoptosis by activation caspase-3, -8, -9, and depolarize the mitochondrial membrane potential. RT-PCR analysis showed that anti-apoptotic protein bcl-2 was down-regulated while pro-apoptotic protein bax was upregulated after MK siRNA transfection. So we conclude that siRNA targeting midkine inhibits gastric cancer cells growth and induces apoptosis involved caspase-3, 8, 9 activation and mitochondrial depolarization.

In our study, 100 nM MK siRNA decreased MK production in BGC823 and SGC7901 human gastric carcinoma cells to about 70% of that in control cultures (Figure 1b). The growth of BGC823 and SGC7901 cells and their colony formation in plate were inhibited after MK siRNA transfection, whereas no effects were observed in the negative control siRNA. The results were in agreement with Takei et al's works [12, 13]. However, in their works, 0.5 mM MK morpholino antisense oligomer was transfected into PC-3 (human prostate carcinoma cell line) and SW 620 (human colon carcinoma cell line) and 5 uM MK antisense oligodeoxynucleotide was transfected into CMT-93 (mouse rectal carcinoma cell line). The mechanism of action of ODNs is that net negatively charged antisense oligodeoxynucleotide elicit RNAse H-mediated cleavage of the target mRNA. While the mechanism of RNAi is that siRNA complementary to the target RNA becomes incorporated into a muti-protein complex (RISC), and leads to degradation of the entire mRNA; the antisense siRNA can be recycled [24]. Because siRNA can be recycled, in order to reaching to similar inhibition effect the dosage of siRNA will be lower than antisense oligodeoxynucleotide. Our results showed that low dosage of anti-MK siRNA can inhibit gastric cancer cell viability (Figure 2), These indicate that MK is relative to cancer cell growth, and MK can act as cancer therapeutic target. MK siRNA might be with potential therapeutic utility for the treatment of gastric cancers.

Midkine can act as antiapoptotic factor in carcinoma cells, and our study showed that anti-MK siRNA can inhibit gastric cancer cell viability, so we investigated the effects of MK siRNA transfection on cell apoptosis. After MK siRNA transfection, compared with parental cells and negative siRNA transfected cells, the percentages of PI positive cells increased about 25 and 30% in BGC823 and SGC7901 cells, respectively (Figure 3); the percentage of Annexin V positive cells was higher than the percentage in parental cells (Figure 4); the percentage of Rhodamine123 positive cells increased about 25 and 30% in BGC823 and SGC7901 cells, respectively (Figure 5). It is indicated that MK siRNA inducing cancer cell apoptosis is relative to mitochondrial depolarization.

The bcl-2 family proteins have a central role in controlling mitochondria apoptosome-mediated apoptotic pathway; the Bcl-2/Bcl-Xl subfamily proteins inhibit apoptosis, while the Bax/Bak subfamily proteins promote cell death [25]. In our study, we detected the mRNA expression level of bcl-2 and bax after MK siRNA transfection, the results showed that the expression of bax was upregulated and the expression of bcl-2 was downregulated after inhibiton of MK expression by MK siRNA (Figure 6). Bcl-2 members form channels that facilitate protein transport and interact with other mitochondrial proteins such as the voltage dependent anion channel, and also induce rupture of the outer mitochondrial membrane. The mitochondrial permeability transition is an important step in this pathway. During this process, the electrochemical gradient across the mitochondrial membrane collapses. The collapse is thought to

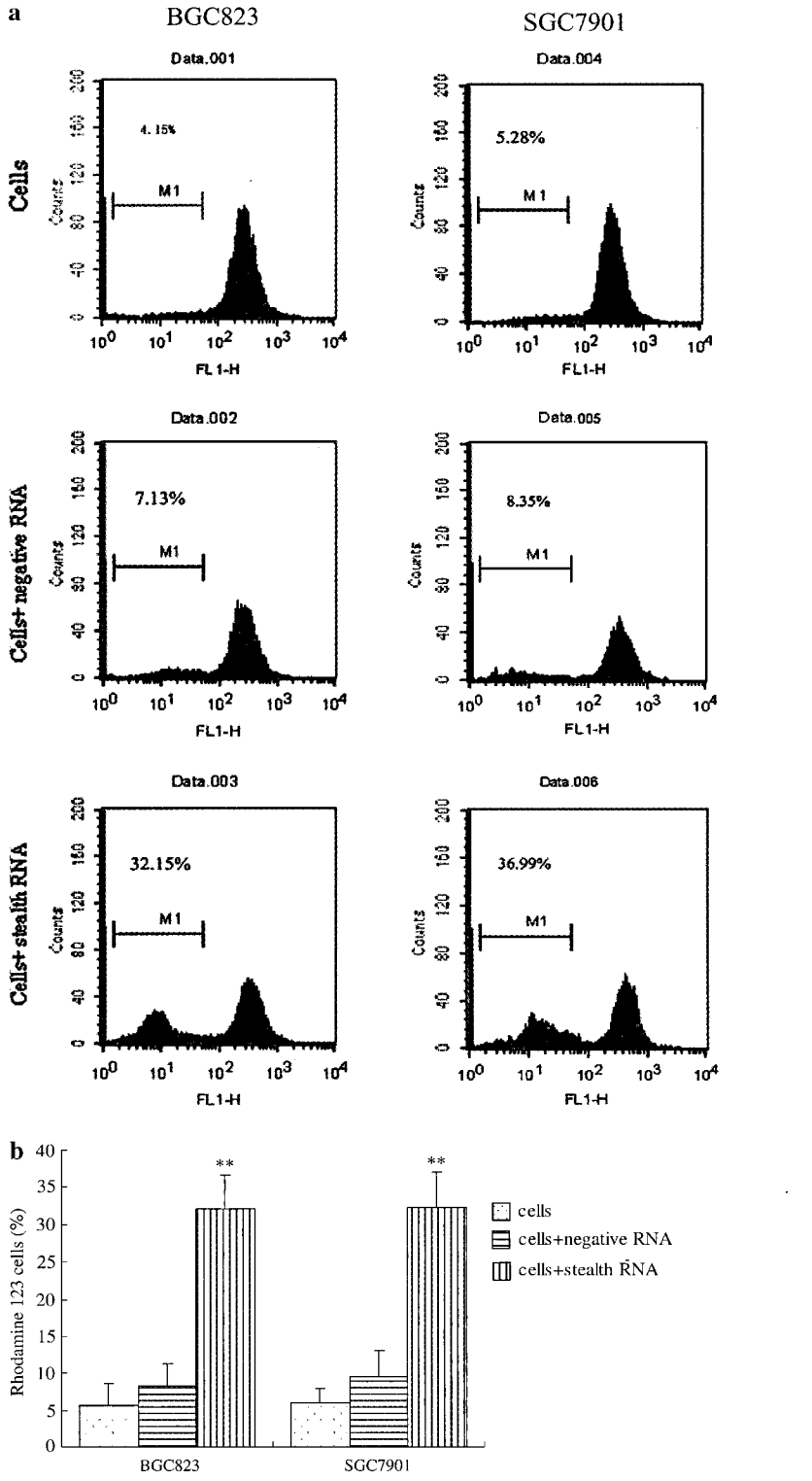
a
BGC823
SGC7901
Cells
Cells+ negative RNA
Cells+ stealth RNA
Data.001
Data.004
Data.002
Data.005
Data.003
Data.006
4.15%
5.28%
7.13%
8.35%
32.15%
36.99%
M1
Counts
FL1-H
b
Rhodamine 123 cells (%)
cells
cells+negative RNA
cells+stealth RNA
BGC823
SGC7901
**

◀ *Figure 5.* Changes in the mitochondrial transmembrane potential detected with rhodamine 123. BGC823 and SGC7901subjected to 72 h after transfection then stained with rhodamine 123 for 30 min at 37°C and was determined by flow cytometry. 10,000 cells were acquired for each sample. (a) The reduced fluorescence of rhodamine 123 was determined as the reduced mitochondrial transmembrane potential in histogram. Data are representative of three experiments. (b) Graph shows the percentages of Rhodamine123 positive cells which represent the mean ± S.E.M from three independent experiments. $^{**}p < 0.01$ versus control.

occur in the formation of pores in the mitochondria by dimerized Bax or activated Bid, Bak, or Bad proteins [26]. Activation of these pro-apoptotic proteins is accompanied by the release of cytochrome c from mitochondria into the cytoplasm and promotes the oligomerisation of cytochrome c/APAF1/procasase9 complexes (apoptosome) which activates procasase3 and leads to the induction of apoptosis. Cytochrome *c* is not the only mitochondrial protein involved in the activation of caspases, Pro-caspases 2, 3, 8, 9 are also involved [22, 23]. In Ohuchida's work, MK pretreatment resulted in the suppression of TRAIL/ActD-mediated apoptosis in HepG2 cells, by inhibiting caspase-3 activity, but caspase-8 activity was not affected [27]. In our study, the results indicated that after MK siRNA transfection, compared with parental cells and cells transfected with negative RNA, the release of cytochrome c from the mitochondria into cytosol was increased (Figure 7), and the caspase-3, 8 and 9 were all activated in BGC823 cell and SGC7901 cells. The activity of caspase-3 and caspase-9 were stronger than that of caspase-8 (Figure 8). It indicated that apoptosis of MK siRNA transfected cells might be mediated by the mitochondria-apoptosome-mediated pathway. The down-regulated expression of bcl-2 and up-regulated expression of bax decreased mitochondrial membrane potential, and led to release of cytochrome c, and activated caspase-3, 8 and 9, especially caspase-3 and caspase-9, at last induce the apoptosis of the cells.

In summary, MK siRNA can inhibit the proliferation and induce the apoptosis of gastric

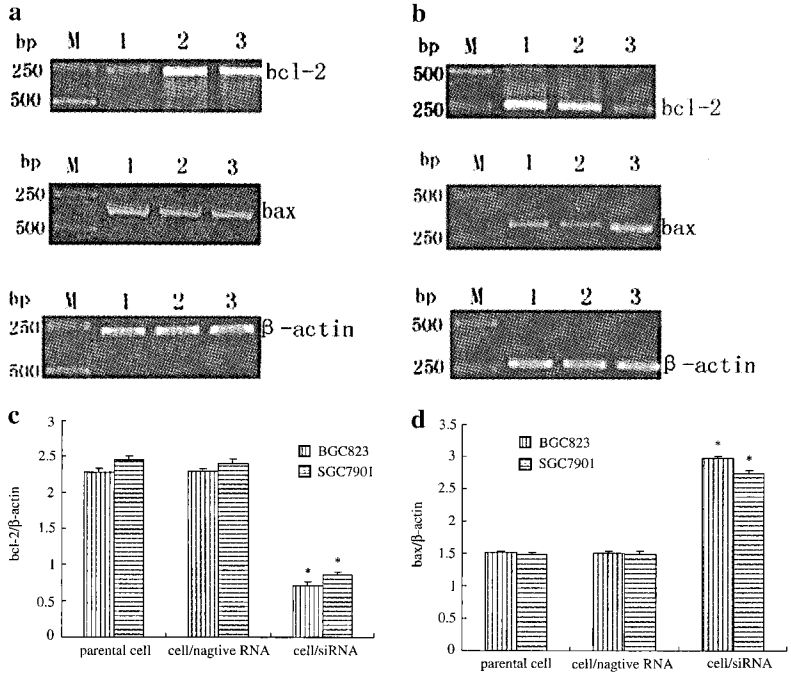

Figure 6. Analysis of bcl-2 and bax mRNA expression level by RT-PCR. (a) The representative agarose gel electrophoresis of three independent experiments is shown. M: DL-2000 (TaKaRa); Lane 1: BGC823 transfected with 100 nM MK siRNA; lane 2: BGC823 transfected with 100 nM negative siRNA; lane 3: parent BGC823; (b) lane 1: parent SGC7901; lane 2: SGC7901 transfected with 100 nM negative siRNA; lane3: SGC7901 transfected with 100 nM MK siRNA. (c) Densitometric analysis of bcl-2. (d) Densitometric analysis of bax. The intensity of the band was scanned. The quotient of MK / β-actin gene was calculated. The data shown are the average of three independent experiments including cDNA synthesis and PCR analysis. The results are shown as mean ± S.E. from three representative independent experiments. $^{*}p < 0.05$ versus Control.

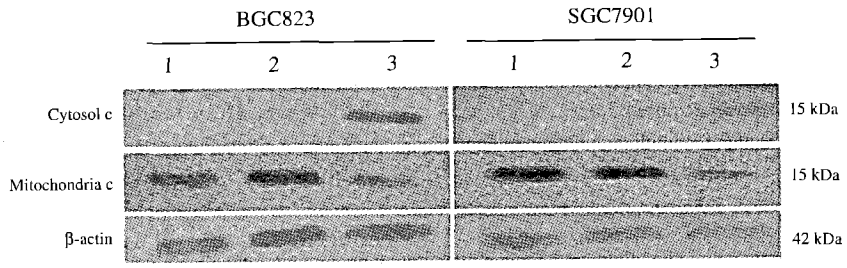

Figure 7. The release of cytochrome c in BGC823 and SGC7901 cells after transfection with anti-MK siRNA. Lane 1: parent cells BGC823; Lane 2: cells transfected with 100 nM negative siRNA; Lane 3: cells transfected with 100 nM MK siRNA.

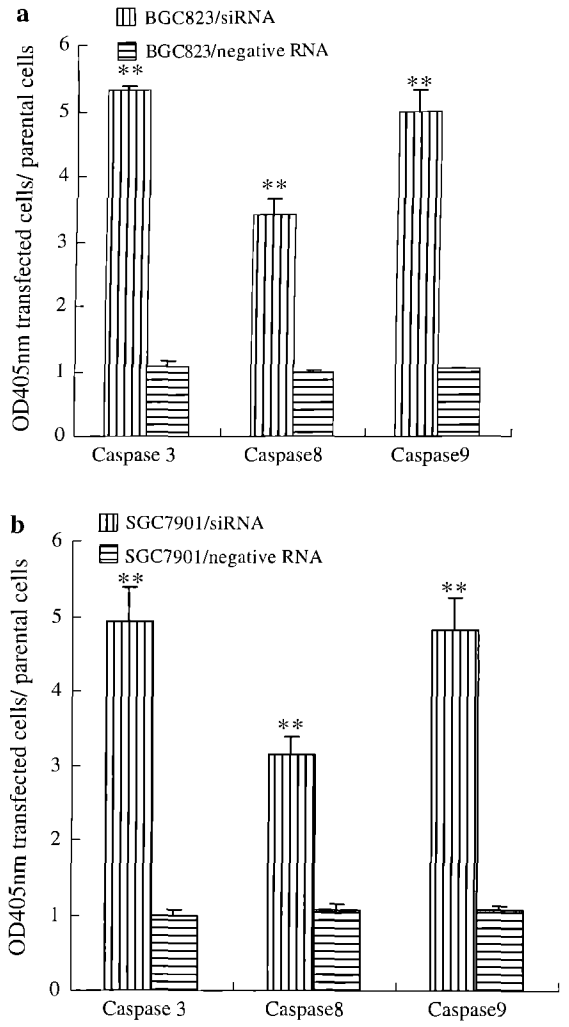

Figure 8. Colorimetric assay for caspase-3, -8, -9 activities at 72 h after transfection. (a) BGC823; (b) SGC7901. Data are means ± SE from three independent experiments. $^{**}p < 0.01$ versus control.

cancer, so MK siRNA may possess potential therapeutic utility for the treatment of gastric cancers. In the future, the stably expression plasmid of short interfering RNAs should be constructed to study its tumor suppressive effect on gastric carcinoma growth *in vivo*.

Acknowledgements

This work was supported by the Scientific Research Foundation of Graduate School of Nanjing University, the Foundation for Key Program of Ministry of Education, China (Grant No. 02111) and the 985-II Program of Nanjing University.

References

1. Kadomatsu K. and Muramatsu T., Midkine and pleiotrophin in neural development and cancer. Cancer Lett. 2: 127–143, 2004.
2. Muramaki M., Miyake H., Hara I. and Kamidono S., Introduction of midkine gene into human bladder cancer cells enhances their malignant phenotype but increases their sensitivity to antiangiogenic therapy. Clin. Cancer Res. 9: 5152–5160, 2003. ,
3. Tsutsui J., Kadomatsu K., Matsubara S., Nakagawara A., Hamanoue M. *et al, A new family of heparin-binding growth/differentiation factors: increased midkine expression in Wilm's* tumor and other human carcinomas. *Cancer Res. 53*(6) 1281–1285, 1993.
4. Aridome K., Tsutsui J., Takao S., Kadomatsu K., Ozawa M., Aikou T. and Muramatsu T., Increased midkine gene expression in human gastrointestinal cancers. Jpn. J. Cancer Res. 86(7) 655–661, 1995.
5. Ikematsu S., Okamoto K., Yoshida Y. *et al, High levels of urinary midkine in various cancer patients. Biochem. Biophys. Res. Commun. 306*(2) 329–332, 2003.
6. Ikematsu S., Yano A., Aridome K. *et al, Serum midkine levels are increased in patients with various types of carcinomas. Br. J. Cancer. 83*(6) 701–706, 2000.
7. Obata Y., Kikuchi S., Lin Y. *et al, Serum midkine concentrations and gastric cancer. Cancer Sci. 96*: 54–56, 2005.
8. Song X., Muramatsu H., Aridome K., Aikou T., Koide N., Tsuji T. and Muramatsu T., The serum level of midkine,

heparin-binding growth factor, as a tumor maker. Biomed. Res. 18: 375–381, 1997.
9. Kaifi J.T., Fiegel H.C., Rafnsdottir S.L. *et al, Midkine as a prognostic marker for gastrointestinal stromal tumors. J. Cancer Res. Clin. Oncol. 133*: 431–435, 2007.
10. Huang Y.L., Cao G.C., Wang H., Wang Q.L. and Hou Y.Y., The expression and location of midkine in gastric carcinomas of Chinese patients. Cell Mol. Immunol. 4(2) 135–140, 2007.
11. Inoh K., Muramatsu H., Torii S., Ikematsu S., Oda M., Kumai H., Sakuma S., Inui T., Kimura T. and Muramatsu T., Doxorubicin-conjugated anti-midkine monoclonal antibody as a potential anti-tumor drug. Jpn. J. Clin. Oncol. 36: 207–211, 2006.
12. Takei Y., Kadomatsu K., Matsuo S., Itoh H., Nakazawa K., Kubota S. and Muramatsu T., Antisense oligodeoxynucleotide targeted to midkine, a heparin-binding growth factor, suppresses tumorigenicity of mouse rectal carcinoma cells. Cancer Res. 61: 8486–8491, 2001.
13. Takei Y., Kadomatsu K., Yuasa K., Sato W. and Muramatsu T., Morpholino antisense oligomer targeting human midkine: its application for cancer therapy. Int. J. Cancer 114: 490–497, 2005.
14. Banno H., Takei Y., Muramatsu T., Komori K. and Kadomatsu K., Controlled release of small interfering RNA targeting midkine attenuates intimal hyperplasia in vein grafts. J. Vasc. Surg. 44: 633–641, 2006.
15. Sato W., Takei Y., Yuzawa Y., Matsuo S., Kadomatsu K. and Muramatsu T., Midkine antisense oligodeoxyribonucleotide inhibits renal damage induced by ischemic reperfusion. Kidney Int. 67: 1330–1339, 2005.
16. Dorsett Y. and Tuschl T., siRNAs: application in functional genomics and potential therapeutics. Nat. Rev. Drug Discov. 3: 318–329, 2004.
17. Soutschek J., Akinc A., Bramlage B., Charisse K., Constien R., Donoghue M., Elbashir S., Geick A., Hadwiger P., Harborth J. *et al, Therapeutic silencing of an endogenous gene by systemic administration of modified siRNAs. Nature 432*: 173–178, 2004.
18. Caplen N.J., Down regulating gene expression: the impact of RNA interference. Gene Ther. 11: 1241–1248, 2004.
19. Ishiyama M., Miyazono Y., Sasamoto K., Ohkura Y. and Ueno K., A highly water-soluble disulfonated tetrazolium salt as a chromogenic indicator for NADH as well as cell viability. Talanta 44: 1299–1305, 1997.
20. Bai J., Rodriguez A.M., Malendez J.A. and Cederbaum A.I., Overexpression of catalase in cytosolic or mitochondrial compartment protects HepG2 cells against oxidative injury. J. Biol. Chem. 274: 26217–26224, 1999.
21. Pathak N. and Khandelwal S., Influence of cadmium on murine thymocytes: potentiation of apoptosis and oxidative stress. Toxicol. Lett. 165: 121–132, 2006.
22. Parone P.A., James D. and Martinou J.C., Mitochondria: regulating the inevitable. Biochimie 84: 105–111, 2002.
23. Wei H. and John J.K., Anticancer therapy targeting the apoptotic pathway. Lancet Oncol. 4: 721–729, 2003.
24. Lisa J.S. and John J.R., Approaches for the sequence-specific knockdown of mRNA. Nat. Biotechnol. 21: 1457–1465, 2003.
25. Liu J.J., Lin D.J., Liu P.Q., Huang M., Li X.D. and Huang R.W., Induction of apoptosis and inhibition of cell adhesive and invasive effects by tanshinone IIA in acute promyelocytic leukemia cells in vitro. J. Biomed. Sci. 13: 813–823, 2006.
26. Mayer B. and Oberbauer R., Mitochondrial regulation of apoptosis. News Physiol. Sci. 18: 89–94, 2003.
27. Ohuchida T., Okamoto K., Akahane K., Higure A., Todoroki H., Abe Y. and Kikuchi M., Midkine protects hepatocellular carcinoma cells against TRAIL-mediated apoptosis through down-regulation of caspase-3 activity. Cancer 100: 2430–2436, 2004.